

# Role of Size and Shape on Biofilm Eradication for Nitric Oxide-Releasing Silica Nanoparticles

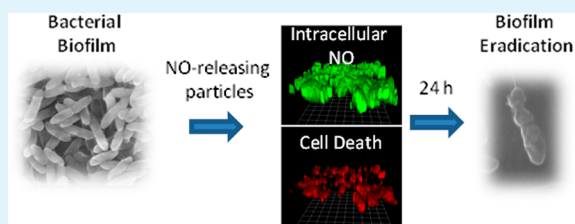
Danielle L. Slomberg, Yuan Lu, Angela D. Broadnax, Rebecca A. Hunter, Alexis W. Carpenter, and Mark H. Schoenfisch\*

Department of Chemistry, University of North Carolina at Chapel Hill, Chapel Hill, North Carolina 27599, United States

## S Supporting Information

**ABSTRACT:** Nitric oxide (NO), a reactive free radical, has proven effective in eradicating bacterial biofilms with reduced risk of fostering antibacterial resistance. Herein, we evaluated the efficacy of NO-releasing silica nanoparticles against Gram-negative *Pseudomonas aeruginosa* and Gram-positive *Staphylococcus aureus* biofilms as a function of particle size and shape. Three sizes of NO-releasing silica nanoparticles (i.e., 14, 50, and 150 nm) with identical total NO release ( $\sim 0.3 \mu\text{mol}/\text{mg}$ ) were utilized to study antibiofilm eradication as a function of size. To observe the role of particle shape on biofilm killing, we varied the aspect ratio of the NO-releasing silica particles from 1 to 8 while maintaining constant particle volume ( $\sim 0.02 \mu\text{m}^3$ ) and NO-release totals ( $\sim 0.7 \mu\text{mol}/\text{mg}$ ). Nitric oxide-releasing particles with decreased size and increased aspect ratio were more effective against both *P. aeruginosa* and *S. aureus* biofilms, with the Gram-negative species exhibiting the greatest susceptibility to NO. To further understand the influence of these nanoparticle properties on NO-mediated antibacterial activity, we visualized intracellular NO concentrations and cell death with confocal microscopy. Smaller NO-releasing particles (14 nm) exhibited better NO delivery and enhanced bacteria killing compared to the larger (50 and 150 nm) particles. Likewise, the rod-like NO-releasing particles proved more effective than spherical particles in delivering NO and inducing greater antibacterial action throughout the biofilm.

**KEYWORDS:** nitric oxide, silica nanoparticles, particle size, particle shape, antibacterial, antibiofilm



## INTRODUCTION

The prevalence of bacteria in clinical settings continues to pose a great challenge in treating and eradicating nosocomial (hospital-acquired) infections, with an estimated 1.7 million infections resulting in  $\sim 99\,000$  deaths in the United States alone each year.<sup>1,2</sup> Most infections are the result of biofilm-based bacteria that irreversibly adhere to a surface and secrete an exopolysaccharide (EPS) matrix.<sup>3</sup> Bacteria utilize the EPS matrix to retain nutrients and impede the diffusion of antibacterial agents.<sup>2,4</sup> Antibiotic-inactivating enzymes, anoxic regions, and the differentiation of cell subpopulations into a more resistant, dormant metabolic state<sup>4</sup> are also employed by the biofilm bacteria to further prevent eradication. As a result, biofilm-based bacteria exhibit increased resistance to treatment and are less susceptible to antibacterial agents compared to planktonic suspensions.<sup>2,5–7</sup> In turn, complete eradication of bacterial biofilms is complex and often not feasible.<sup>1,8,9</sup>

Ideally, implant-associated infections would be controlled by eliminating initial bacteria attachment to a surface and thus preventing biofilm formation of adherent cells.<sup>3</sup> However, superhydrophobic,<sup>10</sup> heparin-coated,<sup>11</sup> and antibacterial-doped substrates<sup>12,13</sup> have not proven effective clinically in reducing infection rates.<sup>3</sup> Researchers have thus turned to more aggressive strategies involving the active release of antibacterial agents.<sup>14</sup> Nitric oxide (NO), a diatomic free radical, serves a number of roles in the body, including the immune response to

pathogens, with antibacterial properties via oxidative and nitrosative stresses when sustained at mid-pM or higher concentrations.<sup>15–17</sup> The effects of NO release on bacterial biofilms are generally concentration-dependent, with biofilm dispersal occurring at low NO concentrations ( $\sim \text{nM}$ ) and killing of the embedded bacteria at higher concentrations ( $\sim \mu\text{M}$ ).<sup>18–20</sup> Barraud et al. reported NO-mediated dispersal of *Pseudomonas aeruginosa* biofilms with exposure to 25–500 nM sodium nitroprusside, after which the bacteria were more susceptible to antibacterials (i.e., tobramycin, hydrogen peroxide, and sodium dodecyl sulfate).<sup>18</sup> At greater NO-release levels (total release  $\sim 10 \mu\text{mol}$  NO) using an enzymatic gaseous NO-releasing dressing, Sulemankhil et al. reported the eradication of *Acinetobacter baumannii*, methicillin-resistant *Staphylococcus aureus*, and *Pseudomonas aeruginosa* biofilms (6 h exposure).<sup>19</sup>

Due to enhanced delivery of NO compared to small molecule NO donors, our lab and others have focused on the synthesis of macromolecular NO donors including silica, metallic nanoparticles, and dendrimers.<sup>21</sup> For example, N-

**Special Issue:** New Frontiers and Challenges in Biomaterials

**Received:** July 2, 2013

**Accepted:** August 20, 2013

**Published:** September 5, 2013



diazoniumdiolate-modified silica nanoparticles were developed to deliver large NO payloads and kill planktonic bacteria.<sup>21,22</sup> Using such scaffolds, Hetrick et al. reported the bacterial killing property of *N*-diazoniumdiolate-modified silica nanoparticles (~100 nm) against *Pseudomonas aeruginosa*, *Escherichia coli*, *Staphylococcus aureus*, *Staphylococcus epidermidis*, and *Candida albicans* biofilms.<sup>20</sup> Nitric oxide released from the particles (~61  $\mu\text{mol}/\text{mL}$ ) eradicated >99% of the biofilm-embedded bacteria. Selective tuning of the physicochemical properties of NO-releasing silica nanoparticles to enhance killing of bacterial biofilms has not been investigated, although initial work with planktonic bacteria indicates that both silica nanoparticle size and shape are important.<sup>23,24</sup> Carpenter et al. reported improved killing of *Pseudomonas aeruginosa* with smaller (50 nm) silica particles.<sup>23</sup> Similarly, silica nanoparticle size proved important in *C. albicans* surface adhesion, with reduced attachment and growth in the presence of smaller particles ( $\leq 14$  nm).<sup>25</sup> Lu et al. observed improved biocidal efficacy for rod-like particles vs silica spheres.<sup>24</sup> Herein, we investigate the role of NO-releasing silica nanoparticle size (i.e., 14, 50, 150 nm) and shape (i.e., aspect ratio 1, 4, and 8) on the eradication of established Gram-negative *Pseudomonas aeruginosa* and Gram-positive *Staphylococcus aureus* biofilms. Such studies are important since >99% of all bacteria exist in a biofilm state and such communities are increasingly difficult to treat.<sup>2</sup>

## ■ EXPERIMENTAL PROCEDURES

**Materials.** Tetraethylorthosilicate (TEOS), *N*-(6-aminohexyl)-aminopropyltrimethoxysilane (AHAP), and *N*-(2-aminoethyl)-3-amino-isobutyl-dimethyl-methoxysilane (AEAI) were purchased from Gelest (Morrisville, PA). Cetyltrimethylammonium bromide (CTAB) was obtained from Acros Organics (Geel, Belgium). Ethanol (EtOH), ammonium hydroxide (28 wt %), Tris base, and Tris hydrochloride were purchased from Fisher Scientific (Fair Lawn, NJ). Organosilicasol MT-ST silica particles (14 nm) in methanol were obtained from Nissan Chemical Corporation (Houston, TX). Tetramethylorthosilicate (TMOS), sodium methoxide (5.4 M in methanol), sulfanilamide, *N*-1-naphthylethylenediamine dihydrochloride, rhodamine B isothiocyanate (RITC), propidium iodide (PI), fetal bovine serum (FBS), Dulbecco's Modified Eagle's Medium (DMEM), phenazine methosulfate (PMS), 3-(4,5-dimethylthiazol-2-yl)-5-(3-carboxymethoxyphenyl)-2-(4-sulfophenyl)-2H-tetrazolium inner salt (MTS), trypsin, phosphate buffered saline (PBS) used for cell culture, and Pen Strep solution (10,000 u/mL penicillin, 10,000  $\mu\text{g}/\text{mL}$  streptomycin) were purchased from the Sigma Aldrich Corp. (St. Louis, MO). Tryptic soy broth (TSB) and tryptic soy agar (TSA) were obtained from Becton, Dickinson, and Company (Franklin Lakes, NJ). *Pseudomonas aeruginosa* (ATCC #19143) and *Staphylococcus aureus* (ATCC #29231) were obtained from the American Type Culture Collection (Manassas, VA). The Centers for Disease Control and Prevention (CDC) bioreactor was purchased from BioSurface Technologies Corporation (Bozeman, Montana). Medical grade silicone rubber (1.45 mm thick) was purchased from McMaster Carr (Atlanta, GA) and doubled in thickness using Superflex Clear RTV silicone adhesive sealant (Loctite, Westlake, OH) to fabricate coupons to fit the CDC reactor (thickness ~4 mm and diameter ~12.7 mm). L929 mouse fibroblasts (ATCC #CCL-1) were purchased from the University of North Carolina Tissue Culture Facility (Chapel Hill, NC). Syto 9 green fluorescent nucleic acid stain was purchased from Life Technologies (Grand Island, NY). 4,5-Diaminofluorescein diacetate (DAF-2 DA) was purchased from Calbiochem (San Diego, CA). Nitric oxide (NO) was purchased from Praxair (Bethlehem, PA). Argon (Ar) gas was obtained from Airgas National Welders (Raleigh, NC). A Millipore Milli-Q UV Gradient A10 System (Bedford, MA) was used to purify distilled water to a final resistivity of 18.2 M $\Omega$  cm and a total organic content of  $\leq 6$  parts per billion (ppb). Other

solvents and chemicals were analytical-reagent grade and used as received.

**Synthesis of Silica Nanoparticles.** Three silica nanoparticle systems (i.e., 14, 50, and 150 nm) were utilized to evaluate antibiofilm efficacy over a range of sizes. Secondary amine-functionalized 14 nm silica particles were prepared via surface grafting according to a modified previously reported procedure.<sup>26</sup> Briefly, 600  $\mu\text{L}$  of 14 nm organosilicasol MT-ST particles in methanol (225 mg/mL) and 1 mL of *N*-(6-aminohexyl)aminopropyltrimethoxysilane (AHAP) were added to a stirred solution of EtOH (100 mL) and allowed to react overnight (~18 h) with heating (48  $^{\circ}\text{C}$ ). The particles were collected by adding water to the solution in a 2:1 ratio (v/v) and centrifugation (4696 g for 15 min, 4  $^{\circ}\text{C}$ ). Following collection, the particles were resuspended in EtOH via sonication and collected again by centrifugation. This washing procedure was performed twice. The particles were then dried under vacuum. The 50 nm silica particles were synthesized by adding TEOS (2.28 mL) to a stirred solution of EtOH (110 mL), ammonium hydroxide (4.05 mL), and water (1.74 mL). After 5 h, the 50 nm silica particles were surface-grafted with AHAP by adding an aliquot of the silane (5.02 mL) to the reaction flask and allowing the reaction to proceed overnight (~18 h). The particles were then collected by adding hexane to the solution in a 2:1 ratio (v/v) and centrifugation (4696 g for 15 min, 4  $^{\circ}\text{C}$ ). Following collection, the 50 nm particles were resuspended in EtOH via sonication and collected again by centrifugation. This washing procedure was carried out twice. The particles were then dried under vacuum. Secondary amine-functionalized 150 nm silica particles were synthesized by adding TMOS (0.71 mL) and AHAP (1.17 mL) to a stirred solution of EtOH (59.16 mL), ammonium hydroxide (9.8 mL), and water (27.84 mL). After 2 h, the 150 nm particles were collected via centrifugation (4696 g for 15 min, 4  $^{\circ}\text{C}$ ), washed with EtOH, and dried according to the aforementioned procedure.

Silica particles of three distinct aspect ratios (AR1, AR4, and AR8) were synthesized via a surfactant-templated approach as previously described by varying reaction temperature and ammonia concentration.<sup>24</sup> Elevated temperature (30 vs 20  $^{\circ}\text{C}$ ) was used to increase the aspect ratio of the particles (AR8), while a greater ammonia concentration (1.0 vs 0.5 M) allowed for the synthesis of a more spherical particle (AR1). Of note, cetyltrimethylammonium bromide (CTAB) removal was confirmed via CHN analysis prior to surface grafting. Monoalkoxysilane, *N*-(2-aminoethyl)-3-amino-isobutyl-dimethyl-methoxysilane (AEAI) was then surface grafted onto the particle/rods to impart secondary amine functionality for *N*-diazoniumdiolation as described below.

The 14, 50, and 150 nm silica particles were functionalized with *N*-diazoniumdiolate NO donors by suspending the particles (20 mg) in a 9:1 (v/v) solution of *N,N*-dimethylformamide (DMF) and methanol (MeOH) and adding 37, 25, and 50  $\mu\text{L}$  of 5.4 M sodium methoxide in MeOH for the 14, 50, and 150 nm particles, respectively. Vials of the solution suspensions were then placed in a Parr hydrogenation vessel and stirred. Residual oxygen in the suspensions was removed by purging the vessel with argon (Ar) three times quickly, followed by three longer (10 min) Ar purges. The vessel was then pressurized to 10 atm with purified gaseous NO. The hydrogenation vessel was maintained at 10 atm throughout a 3 day period after which the Ar purging procedure was repeated to remove unreacted NO prior to removal of the vials from the vessel. The *N*-diazoniumdiolated particles were recollected by centrifugation (4696 g for 15 min, 25  $^{\circ}\text{C}$ ), washed three times with EtOH, dried under vacuum, and stored at  $-20$   $^{\circ}\text{C}$  until use. Similarly, *N*-diazoniumdiolate-functionalized AR1, AR4, and AR8 silica particles were prepared by suspending the AEAI-functionalized particles (15 mg) in a 9:1 (v/v) solution of DMF and MeOH, and adding 50  $\mu\text{L}$  of sodium methoxide (5.4 M in MeOH). Vials of the suspensions were placed in the Parr hydrogenation vessel, purged with Ar, exposed to NO, and the resulting particles were recollected and stored following the same protocol.

**Fluorescently Labeled Silica Nanoparticles.** Fluorescently labeled silica nanoparticles were achieved via covalent modification with rhodamine B isothiocyanate (RITC) based on a previously published procedure.<sup>23</sup> The 14, 50, or 150 nm silica particles (50 mg)

were suspended in EtOH (100 mL) with RITC (5 mg) and stirred in the dark for 48 h. Following fluorescent modification, the particles were collected and washed copiously with EtOH using the collection/centrifugation protocol described above. After a clear supernatant was achieved, the particles were dried under vacuum and stored until use.

**Characterization of Nitric Oxide Release.** Size and shape (i.e., aspect ratio) of the particles were determined using transmission electron microscopy (TEM) and scanning electron microscopy (SEM). Transmission electron micrographs of the 14, 50, and 150 nm silica particles were obtained on a JEOL 100 CX II transmission electron microscope (Tokyo, Japan). Scanning electron micrographs of the AR1, AR4, and AR8 silica particles were recorded using a Hitachi S-4700 scanning electron microscope (Tokyo, Japan). Real-time NO-release from the particles was measured using a Sievers 280i Chemiluminescence Nitric Oxide Analyzer (NOA; Boulder, CO). The NO-releasing particles (1 mg) were added to a sample vessel containing 30 mL deoxygenated PBS (pH 7.4, 37 °C). Liberated NO was carried from the sample vessel to the NOA at a flow rate of 70 mL/min. To match the collection rate of the NOA (200 mL/min), we supplied additional nitrogen flow to the sample vessel. Nitric oxide-release measurements were terminated when the levels fell below 10 ppb NO/mg particle. The real-time NO-release data was used to determine the total NO-release duration and half-life ( $t_{1/2}$ ). Total NO storage ( $t[\text{NO}]$ ) was characterized using the Griess assay.<sup>27,28</sup>

**Planktonic Bacterial Assays.** *Pseudomonas aeruginosa* and *Staphylococcus aureus* bacterial cultures were grown from frozen stock (−80 °C) in TSB overnight at 37 °C. An aliquot of the suspension (0.5 mL) was added to fresh TSB (50 mL) and incubated at 37 °C until the bacteria reached midexponential phase ( $\sim 1 \times 10^8$  colony forming units (cfu)/mL) as determined by the optical density at 600 nm ( $\text{OD}_{600}$ ). The relationship between the concentration of the bacteria in suspension and the  $\text{OD}_{600}$  was calibrated for each strain using an Eppendorf BioPhotometer Plus Spectrophotometer (Hamburg, Germany); the colony forming units were enumerated from culture dilutions grown on TSA plates. The bacterial suspension was then centrifuged (3645 g for 10 min, 25 °C), resuspended in PBS, and diluted to  $\sim 1 \times 10^6$  cfu/mL in PBS supplemented with 1% (w/w) glucose, 0.5% (v/v) TSB, and 100 mM Tris for planktonic bactericidal assays.

The minimum bactericidal concentration (MBC) of the NO-releasing silica particles for planktonic *P. aeruginosa* and *S. aureus* was defined as the concentration that resulted in a 3-log reduction in viability versus untreated cells after 24 h. The bacterial suspensions ( $10^6$  cfu/mL) were incubated with NO-releasing particles for 24 h over a range of particle concentrations. After exposure, the samples were diluted, plated on TSA, with counting of resulting colonies to determine viability.

**Bacterial Biofilm Assays.** A CDC bioreactor was used to grow *P. aeruginosa* and *S. aureus* biofilms over 48 h.<sup>29</sup> Growth conditions (e.g., nutrient concentrations, additives, flow rate) were optimized for both the *P. aeruginosa* and *S. aureus* biofilms. Briefly, medical grade silicone rubber substrates were mounted in the coupon holders within the CDC reactor. After autoclaving, the reactor effluent line was clamped and 500 mL sterile 1% (w/v) TSB (*P. aeruginosa* growth) or 10% (w/v) TSB and 0.1% (w/v) glucose (*S. aureus* growth) was added aseptically. Similar to planktonic experiments, *P. aeruginosa* and *S. aureus* bacterial cultures were grown from frozen stock (−80 °C) overnight in TSB at 37 °C, reinoculated, and grown to midexponential phase. The reactor was then inoculated with an aliquot (1 mL) of the resulting  $1 \times 10^8$  cfu/mL bacterial suspension (final concentration  $\sim 2 \times 10^5$  cfu/mL). The completed assembly was incubated at 37 °C for 24 h with stirring (150 rpm). Following this “batch phase” growth, the effluent line was opened and the reactor media was refreshed continuously with 0.33% (v/v) TSB at 6 mL/min (*P. aeruginosa* growth) or 1% (v/v) TSB at 2 mL/min (*S. aureus* growth) for another 24 h to complete growth of the biofilms.

The MBC for biofilm eradication was determined as the concentration of NO-releasing silica particles that resulted in bacterial viability below the limit of detection for the plate counting method ( $2.5 \times 10^3$  cfu/mL).<sup>23</sup> Each strain of bacteria was tested in triplicate

over an optimized concentration range. *P. aeruginosa* and *S. aureus* biofilms grown on silicone rubber substrates were exposed to several concentrations of NO-releasing silica nanoparticles in 3 mL PBS supplemented with 1% (w/w) glucose, 0.5% (v/v) TSB, and 100 mM Tris at 37 °C with slight agitation for 24 h. After 24 h of incubation, the samples were sonicated and vortexed to disrupt the biofilm. Aliquots of the cell/nanoparticle suspensions were diluted in PBS, plated on TSA, and incubated at 37 °C overnight. Bacterial viability was then determined by counting the observed colonies.

**Confocal Microscopy.** *P. aeruginosa* biofilms were grown on glass substrates (Biosurface Technologies) and subsequently exposed to NO-releasing silica nanoparticles (1 mg/mL) in PBS supplemented with DAF-2 DA (10  $\mu\text{M}$ ) and PI (30  $\mu\text{M}$ ) for 15–60 min or RITC-labeled 14 or 150 nm control (i.e., non-NO-releasing) silica nanoparticles (0.1 mg/mL) in PBS supplemented with Syto 9 (10  $\mu\text{M}$ ) for 30 min. Before imaging, the substrates were dipped in PBS to remove excess dye and loosely adhered cells. A Zeiss 510 Meta inverted laser scanning confocal microscope (Carl Zeiss, Thornwood, NY) with a 488 nm Ar excitation laser (2.0% intensity) and a BP 505–530 nm filter was used to obtain DAF-2 and Syto 9 (green) fluorescence images. A 543 nm HeNe excitation laser (25.3% intensity) with a BP 560–615 nm filter was used to obtain PI and RITC (red) fluorescence images. The images were collected using a Zeiss C-apochromat lens (20 $\times$ , 1.2 numerical aperture).

**In vitro Cytotoxicity.** L929 mouse fibroblasts were cultured in DMEM supplemented with 10% (v/v) FBS and 1 wt % Pen Strep solution, and incubated in 5% (v/v)  $\text{CO}_2$  under humidified conditions at 37 °C. After reaching 80% confluency, the cells were trypsinized, seeded onto tissue culture-treated polystyrene 96-well plates at a density of  $3 \times 10^4$  cells/mL and incubated at 37 °C for 48 h. The supernatant was then aspirated prior to adding fresh DMEM (200  $\mu\text{L}$ ) with control (i.e., non-NO-releasing) or NO-releasing nanoparticles to each well. After incubation at 37 °C for 24 h, the supernatant was aspirated and the cells rinsed 3 $\times$  with PBS. A mixture of DMEM/MTS/PMS (105/20/1, v/v/v) (120  $\mu\text{L}$ ) was then added to each well. The absorbance of the resulting colored solution after 1.5 h incubation at 37 °C was quantified at 490 nm using a Thermo Scientific Multiskan EX plate reader (Thermo Fisher Scientific, Inc., Waltham, MA). The mixture of DMEM/MTS/PMS and untreated cells were used as the blank and control, respectively. Cell viability was calculated by taking the ratio of the absorbance of treated to untreated cells after subtracting the absorbance of the blank from each.

## RESULTS AND DISCUSSION

Although several studies have evaluated the effects of metal and metal oxide nanoparticle physicochemical properties on planktonic bacteria killing,<sup>23,24,30–32</sup> most bacteria exist in a biofilm state where the secreted EPS matrix impedes antibacterial agent diffusion and prevents eradication. In turn, the results of such studies must be considered carefully, particularly with respect to antibacterial efficacy. The potential to realize an effective bacterial biofilm killing scaffold using NO-releasing silica nanoparticles warrants a detailed study of particle size and shape on bacterial biofilm eradication.

Since smaller (<200 nm) NO-releasing silica nanoparticles were previously reported to be more bactericidal than larger scaffolds,<sup>23</sup> we initiated experiments using particles spanning 14–150 nm to enable a thorough evaluation of antibiofilm efficacy as a function of particle size.<sup>33,34</sup> The sizes of the as obtained/prepared particles measured by electron microscopy are provided in Table 1. Nitric oxide release was achieved by modifying the particles with *N*-(6-aminohexyl)-aminopropyltrimethoxysilane (AHAP), and reacting the amines with NO. The three particle systems exhibited NO-release half-lives of  $0.15 \pm 0.2$ ,  $0.83 \pm 0.14$ , and  $0.67 \pm 0.06$  h for the 14, 50, and 150 nm particles, respectively, and similar total NO-release durations of  $\sim 4$ –6 h (Table 1).

**Table 1. Particle Size As Determined by Transmission Electron Microscopy (TEM), Total Micromoles NO Released per mg of Particle As Measured by the Griess Assay, and NO-Release Half-Life ( $t_{1/2}$ ) and Total Duration ( $t_d$ ) As Measured by NOA<sup>a</sup>**

| scaffold | size (nm)      | total NO release ( $\mu\text{mol}/\text{mg}$ ) | $t_{1/2}$ (h)   | $t_d^b$ (h)     |
|----------|----------------|--|-----------------|-----------------|
| 14 nm    | 14.8 $\pm$ 2   | 0.24 $\pm$ 0.01                                | 0.15 $\pm$ 0.02 | 4.76 $\pm$ 1.76 |
| 50 nm    | 56.1 $\pm$ 5   | 0.26 $\pm$ 0.02                                | 0.83 $\pm$ 0.14 | 4.34 $\pm$ 1.32 |
| 150 nm   | 139.9 $\pm$ 13 | 0.25 $\pm$ 0.03                                | 0.67 $\pm$ 0.06 | 5.65 $\pm$ 0.80 |

<sup>a</sup>Size measurements are  $n \geq 20$  and NO release is  $n \geq 3$  syntheses.

<sup>b</sup>Duration above 10 ppb/mg.

To study the role of nanoparticle shape on NO-mediated bactericidal action, we synthesized silica particles of varied aspect ratio (AR1, AR4, and AR8) via a surfactant-templating method in which aspect ratio (1.1  $\pm$  0.2, 4.3  $\pm$  0.5, and 8.2  $\pm$  0.6 for the AR1, AR4, and AR8 particles, respectively) was controlled by tuning temperature and ammonia concentration.<sup>24</sup> Similar to the spherical particles, the rod-like scaffolds were surface modified with *N*-(2-aminoethyl)-3-amino-isobutyl-dimethyl-methoxysilane (AEAI), and reacted with NO to obtain NO-releasing AR1, AR4, and AR8 silica particles. To ensure any differences in bactericidal action were the result of shape (i.e., aspect ratio) alone, the overall particle volume ( $\sim 0.02 \mu\text{m}^3$ ) and total NO release ( $\sim 0.7 \mu\text{mol}/\text{mg}$ ) were tuned to be identical for each particle system (Table 2).<sup>24</sup> The three rod-like NO-releasing silica particles (i.e., AR1, AR4, and AR8) exhibited similar NO-release kinetics with NO-release half-lives of  $\sim 0.7$  h and total durations of  $\sim 13$ – $14$  h (Table 2).

**Bactericidal Efficacy against Planktonic Bacteria as a Function of Size and Shape.** Prior to evaluating the biofilm eradication ability of NO-releasing silica particles as a function of size, the bactericidal activity of 14, 50, and 150 nm NO-releasing silica was evaluated against planktonic *P. aeruginosa* and *S. aureus* suspensions. Minimum bactericidal concentration (MBC) assays were carried out over a 24 h period in bacteria solutions containing nutrients (i.e., PBS supplemented with 1% (w/w) glucose, 0.5% (v/v) TSB, and 100 mM Tris) to ensure survival of the bacteria and mimic conditions for the antibiofilm assays. As expected, the smaller 14 and 50 nm particles were more effective against planktonic *P. aeruginosa* compared to the 150 nm silica particles (MBC<sub>24h</sub> of 0.5 mg/mL for the 14 and 50 nm versus 1 mg/mL for 150 nm) (Table 3). Likewise, the 14 nm particles were more effective against planktonic *S. aureus* compared to the larger particles, with an MBC<sub>24h</sub> of 2 versus 4 mg/mL for the 50 and 150 nm particles. We attribute the greater bactericidal NO doses necessary to kill *S. aureus* vs *P. aeruginosa* (0.48–1.0 vs 0.12–0.25  $\mu\text{mol}$  NO/mL) to multiple factors including differential peptidoglycan thicknesses between the Gram-negative and Gram-positive bacteria,<sup>35</sup> varied production of antioxidant enzymes (e.g., superoxide dismutase)

to mitigate the effects of NO,<sup>36</sup> and *S. aureus*' use of NO as a cytoprotection agent.<sup>37</sup> Although Gram-negative bacteria have an outer membrane that may present a barrier to NO diffusion, increased NO doses are likely unnecessary as NO can degrade the lipid membrane through oxidative and nitrosative stresses or diffuse through porins in the outer membrane.<sup>15,38</sup>

The planktonic bactericidal efficacy of the NO-releasing nanorods was evaluated similarly against *P. aeruginosa* and *S. aureus* suspensions. As reported previously in a 4 h assay,<sup>24</sup> the higher aspect ratio AR8 particles were more effective at killing *P. aeruginosa* after 24 h than the AR4 and AR1 scaffolds (MBC<sub>24h</sub> values of 0.125, 0.250, and 0.250 mg/mL for the AR8, AR4, and AR1 particles, respectively) (Table 4).<sup>24</sup> An identical trend in bactericidal action was noted against planktonic *S. aureus* with an MBC<sub>24h</sub> of 0.125 versus 0.500 mg/mL for the AR4 and AR1 particles. Slightly greater NO doses (0.09–0.33  $\mu\text{mol}$  NO/mL) were also required for *S. aureus* killing compared to those for Gram-negative *P. aeruginosa* (0.09–0.17  $\mu\text{mol}$  NO/mL).

**Biofilm Killing Assays as a Function of Size and Shape.** The antibiofilm efficacy of the particles/rods was evaluated next to assess their utility in eradicating bacteria under more clinically relevant conditions. *P. aeruginosa* ( $\sim 3 \times 10^8$  cfu per substrate) and *S. aureus* ( $\sim 3 \times 10^7$  cfu per substrate) biofilms were exposed to NO-releasing 14, 50, and 150 nm silica particles for 24 h in PBS supplemented with 1% (w/w) glucose, 0.5% (v/v) TSB, and 100 mM Tris buffer. Based on the size-dependent efficacy against planktonic bacteria, we hypothesized that the smaller NO-releasing particles would show enhanced biofilm killing compared to the larger particles. As shown in Table 3, the NO-releasing 14 and 50 nm particles proved more effective than the 150 nm particles, with concentrations as low as 6 mg/mL killing *P. aeruginosa* biofilms compared to 10 mg/mL for the 150 nm particles. As in the planktonic assays, the Gram-positive *S. aureus* biofilms required a greater NO dose for eradication compared to the Gram-negative *P. aeruginosa* biofilms, with MBC<sub>24h</sub> values of 10, 12, and 14 mg/mL for the 14, 50, and 150 nm particles, respectively. Overall, the smaller (i.e., 14 nm) silica particles were characterized by more effective killing of both *P. aeruginosa* and *S. aureus* biofilms compared to the 50 and 150 nm particles. The biofilm bactericidal NO doses were  $\sim 10$ – $12\times$  those required for planktonic killing of *P. aeruginosa*, but only  $\sim 3$ – $5\times$  the NO levels required for planktonic killing of *S. aureus*. The increased NO dose necessary for *P. aeruginosa* biofilm eradication compared to *S. aureus* may arise from general differences in biofilm formation, cell density, and the biofilm's propensity to disperse.<sup>18,39,40</sup> Control (i.e., non-NO-releasing) 14, 50, and 150 nm particles did not significantly reduce *P. aeruginosa* biofilm viability ( $<1$  log killing at their respective MBC concentrations). Control 50 and 150 nm particles slightly reduced *S. aureus* biofilm viability at their

**Table 2. Size and Aspect Ratio of Silica Nanorods As Determined by Scanning Electron Microscopy (SEM), Total Micromoles of NO Released per mg of Particle As Measured by the Griess Assay, and NO Release Half-Life ( $t_{1/2}$ ) and Total Duration ( $t_d$ ) As Measured by NOA<sup>a</sup>**

| scaffold | aspect ratio  | length (nm)   | width (nm)   | total NO release ( $\mu\text{mol}/\text{mg}$ ) | $t_{1/2}$ (h)   | $t_d^b$ (h)      |
|----------|---------------|---------------|--------------|--|-----------------|------------------|
| AR1      | 1.1 $\pm$ 0.2 | 312 $\pm$ 26  | 285 $\pm$ 31 | 0.66 $\pm$ 0.14                                | 0.78 $\pm$ 0.10 | 13.20 $\pm$ 1.41 |
| AR4      | 4.3 $\pm$ 0.5 | 736 $\pm$ 49  | 170 $\pm$ 42 | 0.65 $\pm$ 0.04                                | 0.70 $\pm$ 0.09 | 13.53 $\pm$ 1.50 |
| AR8      | 8.2 $\pm$ 0.6 | 1115 $\pm$ 62 | 137 $\pm$ 45 | 0.68 $\pm$ 0.14                                | 0.74 $\pm$ 0.10 | 14.24 $\pm$ 0.23 |

<sup>a</sup>Size measurements are  $n \geq 50$  and NO release is  $n \geq 3$  syntheses. <sup>b</sup>Duration above 10 ppb/mg.

**Table 3. Determination of Planktonic and Biofilm MBCs and Bactericidal NO Doses for NO-Releasing 14, 50, and 150 nm Silica Particles against *P. aeruginosa* and *S. aureus* Biofilms<sup>a</sup>**

| scaffold | <i>P. aeruginosa</i>       |                      |   |                 | <i>S. aureus</i>           |                      |   |                 |
|----------|----------------------------|----------------------|---|-----------------|----------------------------|----------------------|---|-----------------|
|          | MBC <sub>24h</sub> (mg/mL) |                      | bactericidal NO dose ( $\mu\text{mol/mL}$ ) |                 | MBC <sub>24h</sub> (mg/mL) |                      | bactericidal NO dose ( $\mu\text{mol/mL}$ ) |                 |
|          | planktonic <sup>b</sup>    | biofilm <sup>c</sup> | planktonic                                  | biofilm         | planktonic <sup>b</sup>    | biofilm <sup>c</sup> | planktonic                                  | biofilm         |
| 14 nm    | 0.5                        | 6                    | 0.12 $\pm$ 0.01                             | 1.44 $\pm$ 0.06 | 2                          | 10                   | 0.48 $\pm$ 0.02                             | 2.40 $\pm$ 0.10 |
| 50 nm    | 0.5                        | 6                    | 0.13 $\pm$ 0.01                             | 1.56 $\pm$ 0.12 | 4                          | 12                   | 1.0 $\pm$ 0.08                              | 3.12 $\pm$ 0.24 |
| 150 nm   | 1                          | 10                   | 0.25 $\pm$ 0.03                             | 2.50 $\pm$ 0.30 | 4                          | 14                   | 1.0 $\pm$ 0.01                              | 3.50 $\pm$ 0.42 |

<sup>a</sup>Values determined for  $n = 3$  bacteria assays. <sup>b</sup>MBC: Minimum bactericidal concentration resulting in 3-log reduction in bacterial viability. <sup>c</sup>MBC: Minimum bactericidal concentration resulting in bacterial viability below the limit of detection for the plating method ( $2.5 \times 10^3$  cfu/mL).

**Table 4. Determination of Planktonic and Biofilm MBCs and Bactericidal NO Doses for NO-Releasing AR1, AR4, and AR8 Silica Particles against *P. aeruginosa* and *S. aureus* Biofilms<sup>a</sup>**

| scaffold | <i>P. aeruginosa</i>       |                      |   |                 | <i>S. aureus</i>           |                      |   |                 |
|----------|----------------------------|----------------------|---|-----------------|----------------------------|----------------------|---|-----------------|
|          | MBC <sub>24h</sub> (mg/mL) |                      | bactericidal NO dose ( $\mu\text{mol/mL}$ ) |                 | MBC <sub>24h</sub> (mg/mL) |                      | bactericidal NO dose ( $\mu\text{mol/mL}$ ) |                 |
|          | planktonic <sup>b</sup>    | biofilm <sup>c</sup> | planktonic                                  | biofilm         | planktonic <sup>b</sup>    | biofilm <sup>c</sup> | planktonic                                  | biofilm         |
| AR1      | 0.250                      | 8                    | 0.17 $\pm$ 0.03                             | 5.28 $\pm$ 1.12 | 0.500                      | 12                   | 0.33 $\pm$ 0.07                             | 7.92 $\pm$ 1.68 |
| AR4      | 0.250                      | 1                    | 0.16 $\pm$ 0.01                             | 0.65 $\pm$ 0.04 | 0.500                      | 4                    | 0.33 $\pm$ 0.02                             | 2.60 $\pm$ 0.16 |
| AR8      | 0.125                      | 1                    | 0.09 $\pm$ 0.02                             | 0.68 $\pm$ 0.14 | 0.125                      | 4                    | 0.09 $\pm$ 0.02                             | 2.72 $\pm$ 0.56 |

<sup>a</sup>Values determined for  $n = 3$  bacteria assays. <sup>b</sup>MBC: Minimum bactericidal concentration resulting in 3-log reduction in bacterial viability. <sup>c</sup>MBC: Minimum bactericidal concentration resulting in bacterial viability below the limit of detection for the plating method ( $2.5 \times 10^3$  cfu/mL).

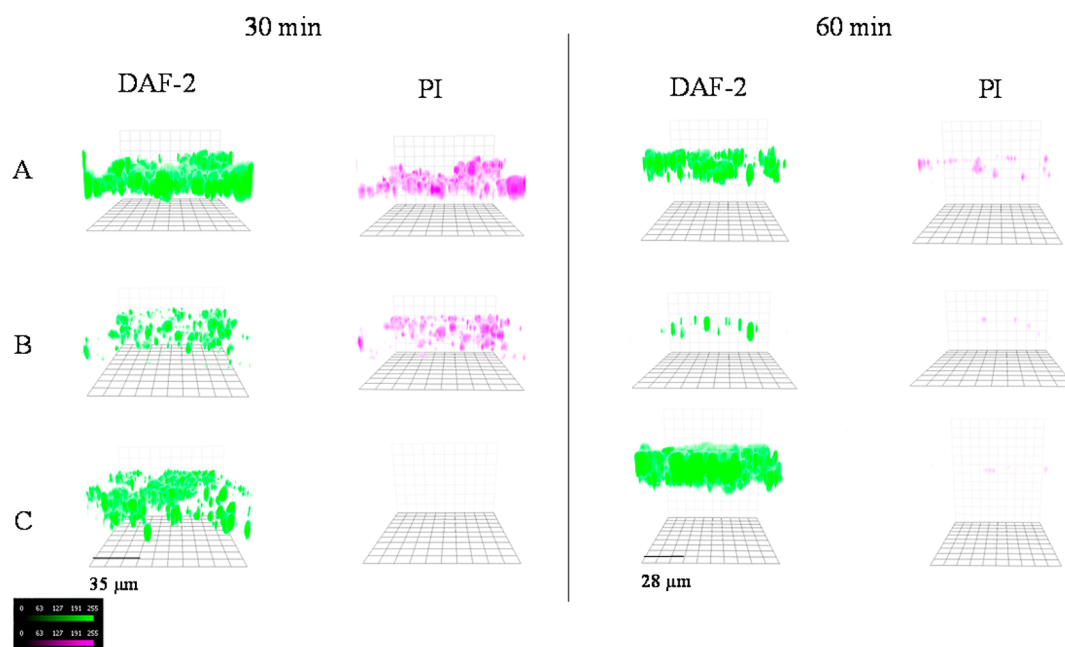


**Figure 1.** Fluorescent images of *P. aeruginosa* biofilm exposed to the same particle concentration (1 mg/mL) and NO dosage ( $\sim 250 \mu\text{mol/L}$ ) of NO-releasing (A) 14, (B) 50, or (C) 150 nm particles for 30 or 60 min. DAF-2 green fluorescence indicates increased intracellular NO and PI red fluorescence indicates compromised cell membranes (i.e., cell death). Fluorescent images were false-colored for clarity.

respective MBCs ( $\sim 1.5$  log), whereas the 14 nm control particles did not affect *S. aureus* cells ( $< 1$  log killing) at 10 mg/mL.

Determination of the role of nanoparticle shape on *P. aeruginosa* and *S. aureus* biofilm killing showed a dependence on aspect ratio similar to that observed in planktonic studies. We hypothesized that higher particle aspect ratios (i.e., AR4 and AR8) would improve NO delivery to bacteria within the biofilm based on the planktonic assays. As shown in Table 4, the 24 h MBCs for the NO-releasing AR8 and AR4 rod-like particles were 1 and 4 mg/mL for *P. aeruginosa* and *S. aureus* biofilms, respectively. The more spherical, NO-releasing AR1 particles

were significantly less effective, with biofilm MBCs of 8 and 12 mg/mL for *P. aeruginosa* and *S. aureus*. The biofilm bactericidal NO doses were  $\sim 4$ – $31\times$  those required for planktonic killing of *P. aeruginosa* and  $\sim 8$ – $30\times$  the NO levels required for planktonic killing of *S. aureus*. As mentioned above, these differences may arise from a variety of biological factors.<sup>18,39,40</sup> Control AR1, AR4, and AR8 particles at their respective biofilm MBCs resulted in negligible reduction in *P. aeruginosa* biofilm viability ( $< 1$  log killing). However, the control scaffolds resulted in a greater reduction in *S. aureus* biofilm viability at their respective biofilm MBCs ( $\sim 2.5$ , 2, and 1.5 log killing for the AR1, AR4, and AR8 particles, respectively) due to the increased

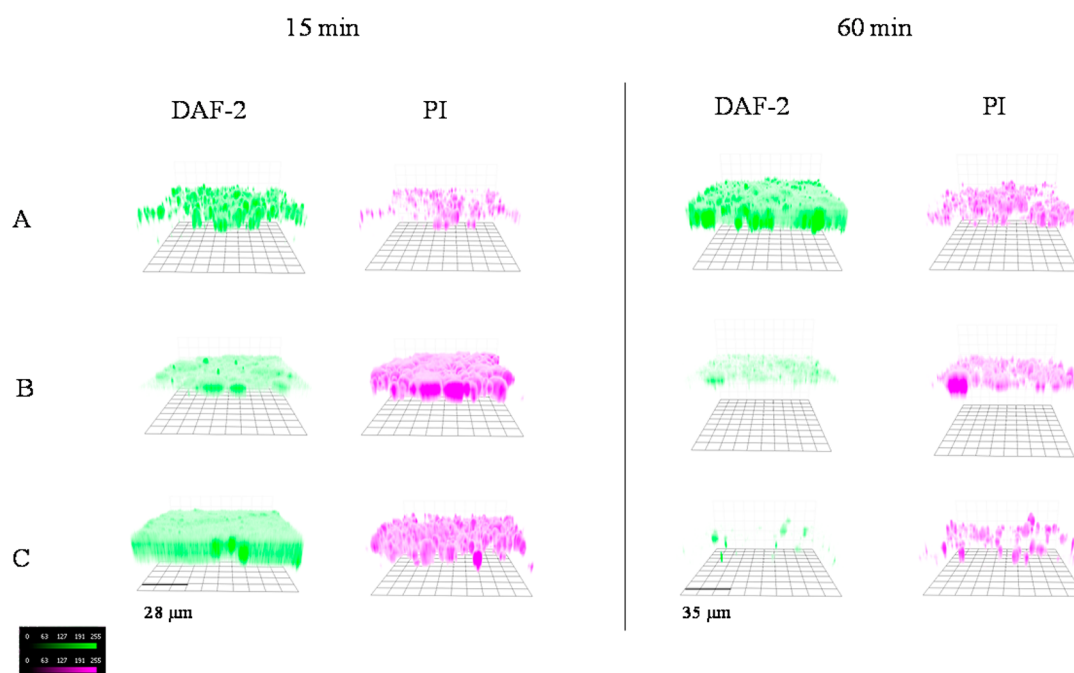


**Figure 2.** Fluorescent images of *P. aeruginosa* biofilm exposed to the same particle concentration (1 mg/mL) and NO dosage ( $\sim 700 \mu\text{mol/L}$ ) of NO-releasing (A) AR1, (B) AR4, or (C) AR8 particles for 15 or 60 min. DAF-2 green fluorescence indicates increased intracellular NO and PI red fluorescence indicates compromised cell membranes (i.e., cell death). Fluorescent images were false-colored for clarity.

scaffold concentration required for eradication. Of note, the MBC values for the NO-releasing 14, 50, and 150 nm silica particles and the AR1, AR4, and AR8 nanorods must be evaluated independently due to differences in NO loading capacity between the particles synthesized via the Stöber method (14, 50, 150 nm) and surfactant-templated approach (AR1, AR4, AR8).<sup>23</sup>

**Confocal Microscopy.** To determine whether the enhanced antibiofilm efficacy observed for smaller particles (i.e., 14 and 50 nm) and higher aspect ratio nanorods (i.e., AR4 and AR8) was due to improved NO delivery, confocal microscopy was used to visualize intracellular NO concentrations and subsequent cell death. Intracellular NO levels were monitored by using 4,5-diaminofluorescein diacetate (DAF-2 DA), a membrane permeable dye that enters the cell and is then hydrolyzed to an impermeable form, DAF-2, via intracellular esterases.<sup>22</sup> Once in the cell, DAF-2 will react with NO to form a green fluorescent derivative, triazolo-fluorescein, resulting in fluorescence that scales with NO concentration. Cell death was visualized using propidium iodide (PI), a dye that only permeates cells with compromised membranes; red fluorescence is produced upon binding with nucleic acids (i.e., DNA and RNA).<sup>41</sup> The build-up of intracellular NO has previously been shown to precede PI signal at sub-MBC particle exposures.<sup>22,42</sup> Intracellular NO levels and cell death were visualized for *P. aeruginosa* biofilms exposed to NO-releasing 14, 50, or 150 nm particles (1 mg/mL in a solution of PBS supplemented with DAF-2 DA and PI) for 30 or 60 min. Of note, intracellular NO levels, cell death, and particle diffusion were not evaluated for *S. aureus* biofilms as killing trends were identical to *P. aeruginosa*. As shown in Figure 1, the DAF-2 (green) signal was greatest for the 14 nm scaffold after incubation with the NO-releasing particles. Such efficient delivery of NO also lead to more rapid cell death for the smallest silica particle NO-release vehicle. Greater intracellular NO (i.e., green fluorescence) was ultimately observed

within the *P. aeruginosa* biofilm after 60 min when using 150 nm NO-releasing particles, despite no visible cell death (red fluorescence). Conversely, the 14 and 50 nm NO-releasing particles effectively dispersed the *P. aeruginosa* biofilm at 60 min,<sup>18</sup> resulting in decreased DAF-2 and PI fluorescence from the few biofilm cells remaining on the substrate (Figure 1).

Intracellular NO levels and cell death were also measured for *P. aeruginosa* biofilms exposed to NO-releasing particles of varied aspect ratio (AR1–AR8). On the basis of confocal experiments with planktonic bacterial suspensions,<sup>24</sup> we hypothesized that increased DAF-2 and PI fluorescence would also be observed for biofilms exposed to higher aspect ratio scaffolds due to improved efficiency of NO delivery. As shown in Figure 2, significant DAF-2 and PI fluorescence were observed throughout the entire *P. aeruginosa* biofilm after exposure to NO-releasing AR4 or AR8 particles at 1 mg/mL for 15 min. Although intracellular NO and cell death were detected for the biofilm exposed to the NO-releasing AR1 particles (1 mg/mL), the fluorescence was localized to small regions of the biofilm (Figure 2). Furthermore, bacteria killing was not observed until 60 min. Conversely, the visibility of the DAF-2 and PI fluorescence decreased for the NO-releasing AR4 and AR8 nanorods at the 60 min time point because of effective *P. aeruginosa* biofilm dispersal.<sup>18</sup>

The role of particle diffusion into the biofilm on bacteria killing was evaluated next to understand if the vehicle or just NO penetrated the biofilms. To carry out this study, the biofilm was stained with a membrane-permeable dye, Syto 9, to enable visualization of the biofilm bacteria.<sup>43</sup> *P. aeruginosa* biofilms were incubated with RITC-labeled 14 and 150 nm control particles (0.1 mg/mL) for 30 min, and then rinsed with PBS to determine whether the particles could penetrate and diffuse into the biofilm. Although particle diffusion into the *P. aeruginosa* biofilm was observed for both the 14 and 150 nm RITC-labeled particles, more significant RITC (red) fluorescence was noted for the 14 nm particles, indicating faster

diffusion for the smaller vs larger particles at 30 min (Figure 3). Comparison of the biofilm regions stained with Syto 9 to those

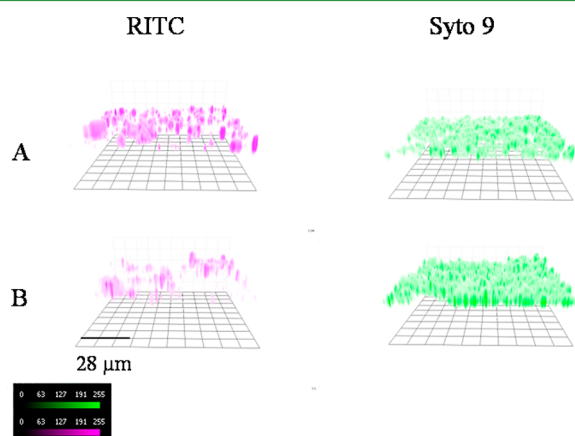


**Figure 3.** Fluorescent images of RITC-modified (A) 14 and (B) 150 nm control particle (0.1 mg/mL) diffusion in *P. aeruginosa* biofilm 30 min after particle addition. Green Syto 9 fluorescence shows biofilm cells. Increased RITC red fluorescence indicates more efficient particle diffusion within biofilm. Fluorescent images were false-colored for clarity.

with RITC fluorescence also confirmed that the 150 nm particles did not adequately penetrate the *P. aeruginosa* biofilm. Of note, the rod-like particles were too large (e.g., AR1 ~300 nm)<sup>44</sup> to readily diffuse into the biofilm, and thus particle–biofilm associations for the nanorods were not visualized.

**In Vitro Cytotoxicity.** The utility of NO-release scaffolds for eradicating biofilms will be governed by both their ability to kill bacteria and not impact healthy host cells or tissue. Previous studies have shown that silica nanoparticle properties (e.g., size) impact cellular response (e.g., morphology, adhesion, and proliferation), further necessitating cytotoxicity evaluation for the NO-release scaffolds presented herein.<sup>45</sup> To assess cytotoxicity, we exposed L929 mouse fibroblasts to NO-releasing and control silica particles. L929 mouse fibroblasts were selected as a model host cell due to their ubiquitous presence in connective tissue.<sup>46</sup> Normalized cell viability was

determined after a 24 h exposure using the MBCs for *P. aeruginosa* and *S. aureus* biofilm eradication. As shown in Figure 4, the NO-releasing 50 nm, AR4, and AR8 particles were nontoxic to the L929 fibroblasts at the MBCs necessary to eradicate *P. aeruginosa* biofilms, with ~30, 22, and 15% reduction in fibroblast viability, respectively. Likewise, control 50 nm, AR4, and AR8 particles did not greatly impact the L929 cells at these concentrations. The cytotoxicity of both control and NO-releasing scaffolds was significantly greater for all other particle systems (e.g., 14 and 150 nm and AR1 particles) at the concentrations ( $\geq 6$  mg/mL) necessary to kill *P. aeruginosa* biofilms. Similarly, Hetrick et al. reported significantly reduced fibroblast viability for both control and NO-releasing silica particles at 8 mg/mL (50 and 70% reductions, respectively).<sup>20</sup> At concentrations necessary to eradicate *S. aureus* biofilms, all particle systems proved cytotoxic (36–71% viability reduction). Overall, the NO-releasing particles decreased fibroblast viability to a greater extent than control systems at the MBCs for *S. aureus* killing, which might be expected given the increased concentration of both scaffold and NO required to eradicate *S. aureus* biofilms. Despite the greater scaffold concentration required to eradicate *S. aureus* biofilms, the fibroblast viabilities for control particles at MBCs for *P. aeruginosa* and *S. aureus* were identical, indicating that the greater NO-release levels play a significant role in the observed toxicity.

## CONCLUSIONS

Despite the moderate cytotoxicity observed for the NO-releasing silica scaffolds at concentrations necessary for biofilm eradication, this work successfully demonstrates the benefits of NO as an antibiofilm agent. Both particle size and shape clearly play important roles in biofilm eradication, with smaller sizes and higher aspect ratios being most effective. The use of NO can effectively eradicate *P. aeruginosa* and *S. aureus* biofilms at concentrations only 3–31x those required for planktonic killing with minimal concern about antibacterial resistance.<sup>47</sup> In contrast, other antibiofilm agents (e.g., antibiotics) exhibit significantly decreased efficacy toward biofilm bacteria and often promote resistance upon repeated exposure.<sup>2</sup> Future work should focus on reducing the toxicity of the NO-release scaffolds to healthy cells and tissue. Additionally, the

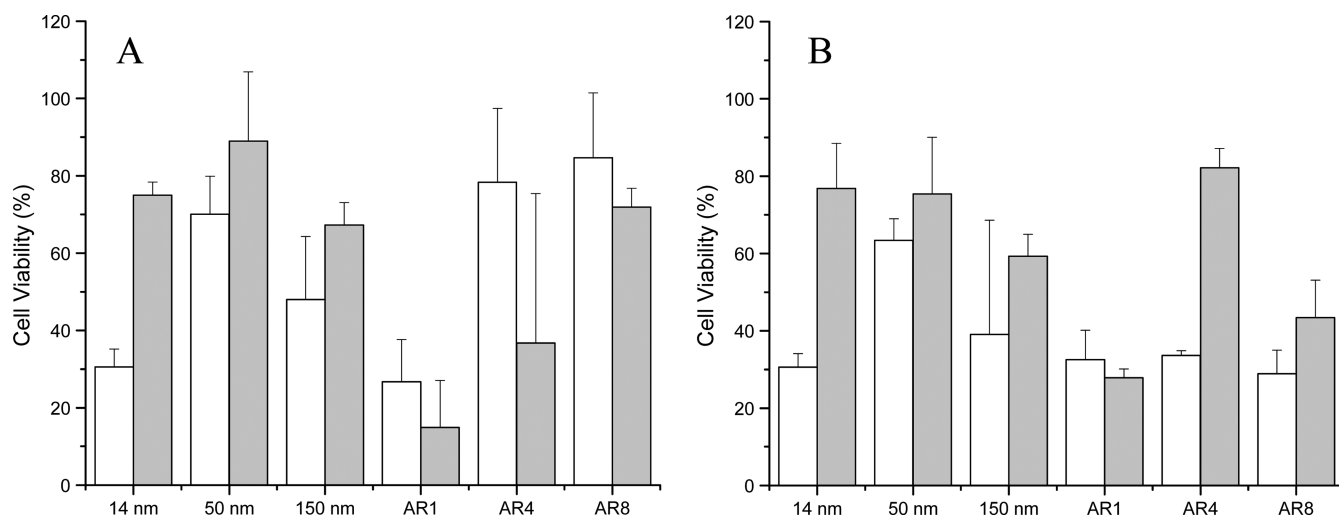


**Figure 4.** Cytotoxicity of NO-releasing (white) and control (gray) silica particles against L929 mouse fibroblasts at MBC concentrations required for (A) *P. aeruginosa* and (B) *S. aureus* biofilm killing as listed in Tables 3 and 4.

combination of NO with other antibacterial agents (e.g., antibiotics, silver) should be explored, as biofilm dispersal by low, nontoxic levels of NO is likely to make the action of current antibiotics more effective.

## ■ ASSOCIATED CONTENT

### Supporting Information

Electron micrographs of 14, 50, and 150 nm silica particles (Figure S1); Electron micrograph of AR1, AR4, and AR8 particles (Figure S2). This material is available free of charge via the Internet at <http://pubs.acs.org>.

## ■ AUTHOR INFORMATION

### Corresponding Author

\*E-mail: [schoenfisch@unc.edu](mailto:schoenfisch@unc.edu). Phone: 919-843-8714. Fax: 919-962-2388.

### Notes

The authors declare the following competing financial interest(s): The corresponding author declares competing financial interest. Mark Schoenfisch is a co-founder, a member of the board of directors, and maintains a financial interest in Novan Therapeutics, Inc. Novan Therapeutics is commercializing macromolecular nitric oxide storage and release vehicles for a variety of clinical indications.

## ■ ACKNOWLEDGMENTS

This work was supported by the National Science Foundation (DMR1104892). The authors thank Dr. Wallace Ambrose of the University of North Carolina at Chapel Hill and the Chapel Hill Analytical and Nanofabrication Laboratory (CHANL) for assistance with SEM preparation and analysis. The authors also thank Dr. Neal Kramarcy of the Michael Hooker Microscopy facility for assistance with confocal experiments.

## ■ REFERENCES

- (1) Bryers, J. D. *Biotechnol. Bioeng.* **2008**, *100*, 1–18.
- (2) Smith, A. W. *Adv. Drug Delivery Rev.* **2005**, *57*, 1539–1550.
- (3) Lindsay, D.; von Holy, A. J. *Hosp. Infect.* **2006**, *64*, 313–325.
- (4) Costerton, J. W.; Stewart, P. S.; Greenberg, E. P. *Science* **1999**, *284*, 1318–1322.
- (5) Anderl, J. N.; Franklin, M. J.; Stewart, P. S. *J. Antimicrob. Chemother.* **2000**, *44*, 1818–1824.
- (6) Nickel, J. C.; Ruseska, I.; Wright, J. B.; Costerton, J. W. *J. Antimicrob. Chemother.* **1985**, *27*, 619–624.
- (7) Cerca, N.; Martins, S.; Cerca, F.; Jefferson, K. K.; Pier, G. B.; Oliveira, R.; Azeredo, J. *J. Antimicrob. Chemother.* **2005**, *56*, 331–336.
- (8) James, G. A.; Swogger, E.; Wolcott, R.; Pulcini, E. d.; Secor, P.; Sestrich, J.; Costerton, J. W.; Stewart, P. S. *Wound Repair Regen.* **2008**, *16*, 37–44.
- (9) Singh, P. K.; Schaefer, A. L.; Parsek, M. R.; Moninger, T. O.; Welsh, M. J.; Greenberg, E. P. *Nature* **2000**, *407*, 762–764.
- (10) Fadeeva, E.; Truong, V. K.; Stiesch, M.; Chichkov, B. N.; Crawford, R. J.; Wang, J.; Ivanova, E. P. *Langmuir* **2011**, *27*, 3012–3019.
- (11) Appelgren, P.; Ransjo, U.; Bindslev, L.; Larm, O. *Lancet* **1995**, *345*, 130–130.
- (12) Chilukuri, D. M.; Shah, J. C. *Pharm. Res.* **2005**, *22*, 563–572.
- (13) Morris, N. S.; Stickler, D. J. *J. Hosp. Infect.* **1998**, *39*, 227–234.
- (14) Hetrick, E. M.; Schoenfisch, M. H. *Chem. Soc. Rev.* **2006**, *35*, 780–789.
- (15) Ignarro, L. J. *Nitric Oxide: Biology and Pathobiology*; Academic Press: San Diego, 2000; p 41–57.
- (16) Fang, F. C. *J. Clin. Invest.* **1997**, *99*, 2818–2825.
- (17) Carpenter, A. W.; Schoenfisch, M. H. *Chem. Soc. Rev.* **2012**, *41*, 3742–3752.
- (18) Barraud, N.; Hassett, D. J.; Hwang, S.-H.; Rice, S. A.; Kjelleberg, S.; Webb, J. S. *J. Bacteriol.* **2006**, *188*, 7344–7353.
- (19) Sulemankhil, I.; Ganopolsky, J. G.; Dieni, C. A.; Dan, A. F.; Jones, M. L.; Prakash, S. *Antimicrob. Agents Chemother.* **2012**, *56*, 6095–6103.
- (20) Hetrick, E. M.; Shin, J. H.; Paul, H. S.; Schoenfisch, M. H. *Biomaterials* **2009**, *30*, 2782–2789.
- (21) Riccio, D. A.; Schoenfisch, M. H. *Chem. Soc. Rev.* **2012**, *41*, 3731–3741.
- (22) Hetrick, E. M.; Shin, J.-H.; Stasko, N. A.; Johnson, C. B.; Wespe, D. A.; Holmuhamedov, E.; Schoenfisch, M. H. *ACS Nano* **2008**, *2*, 235–246.
- (23) Carpenter, A. W.; Slomberg, D. L.; Rao, K. S.; Schoenfisch, M. H. *ACS Nano* **2011**, *5*, 7235–7244.
- (24) Lu, Y.; Slomberg, D. L.; Sun, B.; Schoenfisch, M. H. *Small* **2013**, *9*, 2189–2198.
- (25) Cousins, B. G.; Allison, H. E.; Doherty, P. J.; Edwards, C.; Garvey, M. J.; Martin, D. S.; Williams, R. L. *J. Appl. Microbiol.* **2007**, *102*, 757–765.
- (26) Zhang, H.; Annich, G. M.; Miskulin, J.; Stankiewicz, K.; Osterholzer, K.; Merz, S. I.; Bartlett, R. H.; Meyerhoff, M. E. *J. Am. Chem. Soc.* **2003**, *125*, 5015–5024.
- (27) Coneski, P. N.; Schoenfisch, M. H. *Chem. Soc. Rev.* **2012**, *41*, 3753–3758.
- (28) Hunter, R. A.; Storm, W. L.; Coneski, P. N.; Schoenfisch, M. H. *Anal. Chem.* **2013**, *85*, 1957–1963.
- (29) Goeres, D. M.; Loetterle, L. R.; Hamilton, M. A.; Murga, R.; Kirby, D. W.; Donlan, R. *Microbiol.* **2005**, *151*, 757–762.
- (30) Lu, Z.; Rong, K.; Li, J.; Yang, H.; Chen, R. *J. Mater. Sci.: Mater. Med.* **2013**, *24*, 1465–1471.
- (31) Pal, S.; Tak, Y.-K.; Song, J.-M. *Appl. Environ. Microbiol.* **2007**, *73*, 1712–1720.
- (32) Aminedi, R.; Wadwha, G.; Das, N.; Pal, B. *Environ. Sci. Pollut. Res.* **2013**, *20*, 6521–6530.
- (33) Stöber, W.; Fink, A. *J. Colloid Interface Sci.* **1968**, *26*, 62–69.
- (34) Bogush, G. H.; Tracy, M. A.; Zukoski, C. F., IV. *J. Non-Cryst. Solids* **1988**, *104*, 95–106.
- (35) Silhavy, T. J.; Kahne, D.; Walker, S. *Cold Spring Harb. Perspect. Biol.* **2010**, 1–16.
- (36) Mandell, G. J. *Clin. Invest.* **1975**, *55*, 561–566.
- (37) Gusarov, I.; Nudler, E. *Proc. Natl. Acad. Sci. U.S.A.* **2005**, *102*, 13855–13860.
- (38) Benz, R. *Annu. Rev. Microbiol.* **1988**, *42*, 359–393.
- (39) Boyd, A.; Chakrabarty, A. M. *Appl. Environ. Microbiol.* **1994**, *60*, 2355–2359.
- (40) Boles, B. R.; Horswill, A. R. *PLoS Pathog.* **2008**, *4*, e1000052.
- (41) Boulou, L.; Prevost, M.; Barbeau, B.; Coallier, J.; Desjardins, R. *J. Microbiol. Methods* **1999**, *37*, 77–86.
- (42) Sun, B.; Slomberg, D. L.; Chudasama, S. L.; Lu, Y.; Schoenfisch, M. H. *Biomacromolecules* **2012**, *13*, 3343–3354.
- (43) Boulou, L.; Prevost, M.; Barbeau, B.; Coallier, J.; Desjardins, R. *J. Microbiol. Methods* **1999**, *37*, 77–86.
- (44) Peulen, T.-O.; Wilkinson, K. J. *Environ. Sci. Technol.* **2011**, *45*, 3367–3373.
- (45) Cousins, B. G.; Doherty, P. J.; Williams, R. L.; Fink, J.; Garvey, M. J. *J. Mater. Sci.: Mater. Med.* **2004**, *15*, 355–359.
- (46) Alberts, B.; Johnson, A.; Lewis, J. *Mol. Biol. Cell*, 4th ed.; Garland Science: New York, 2002.
- (47) Privett, B. J.; Broadnax, A. D.; Bauman, S. J.; Riccio, D. A.; Schoenfisch, M. H. *Nitric Oxide* **2012**, *26*, 169–173.